Geophysical Research Letters

Supporting Information for

High-Pressure XAFS Measurements of the Coordination Environments of Fe^{2+} and Fe^{3+} in Basaltic Glasses

Keisuke Ozawa[1], Kei Hirose[1,2], and Yoshio Takahashi[1,3]

[1]Department of Earth and Planetary Science, The University of Tokyo, Tokyo, Japan

[2]Earth-Life Science Institute, Tokyo Institute of Technology, Tokyo, Japan

[3]Institute of Materials Structure Science, High-Energy Accelerator Research Organization, Tsukuba, Ibaraki, Japan

Contents of this file

Experimental Methods

A couple of basaltic glasses were synthesized under reduced and oxidized conditions for the present XAFS measurements. Their chemical compositions and homogeneity were examined with an electron probe microanalyzer (FE-EPMA, JEOL JXA-8530F) (Table S1). They were prepared originally from gel and melted in reducing H_2-CO_2 gas atmosphere at 1473 K (three log units below the QFM buffer) and in air (oxidizing condition) at 1573 K, respectively, for 30 mins. Under the former reducing condition, ferrous iron should be predominant in the glass ($Fe^{2+}/\Sigma Fe = 0.985$) according to Berry et al. (2018). On the other hand, Fe in the latter oxidized glass should be dominated by ferric iron.

We collected both the XANES and EXAFS spectra of these basaltic glasses with increasing pressure at the beamline BL-4A, the Photon Factory, KEK with a beam focused to 5 μm × 5 μm area on a sample by using a K-B mirror system (Figure 1). The spectrum of Fe metal foil was also obtained in a similar manner at ambient condition to calibrate the X-ray energy based on the first inflection point of Fe metal foil at 7111.08 eV following Wilke et al. (2001). Basaltic glasses were compressed to high pressures in a diamond-anvil cell (DAC) using flat anvils with 200–600 μm culet size. In order to minimize X-ray absorption, we employed an X-ray transparent gasket (Merkel & Yagi, 2005) and collected the XAFS spectra under the experimental setting same as described in Ozawa et al. (2021). Measurements were performed near the K-edge of Fe in the fluorescence yield mode. Pressure was measured based on a Raman shift of a diamond anvil above 10 GPa (Akahama & Kawamura, 2004) and the ruby fluorescence method at lower pressures (Mao et al., 1978).

The XAFS scan was performed in an energy range of 7065–7450 eV with 0.3 eV steps for the pre-edge and XANES regions and > 0.9 eV steps for other regions. The spectra were normalized by the average absorbance at the 7200–7300 eV region. Then, the pre-edge feature was obtained by subtracting background that is estimated by using a cubic spline function (Wilke et al., 2001) (Figure 1). After the extraction, the centroid position (intensity-weighted pre-edge position) and the intensity of the pre-edge absorption were calculated (Table S2). We considered uncertainties to be ±10% in pre-edge intensity and ±0.1 eV in the centroid energy following Alderman et al. (2017). The pre-edge intensities at 1 bar for both reduced and oxidized basaltic glasses obtained here in the fluorescence yield mode are comparable to those measured in the transmission mode in Wilke et al. (2005). It indicates that the thickness effect on the pre-edge intensity is negligible compared to the uncertainty in the present measurements.

EXAFS spectra were analyzed by the REX2000 software (Rigaku Co. Ltd.) The k^3-weighted EXAFS oscillation was extracted from each spectrum, and Fourier transformed within the k-range of 2.6–8.4 $Å^{-1}$ to the radial structure functions. In order to extract information on the nearest neighbors of Fe atoms from the radial structural function, the first-neighbour shell EXAFS was filtered out using Hanning window function. The filtered radial structural functions were back-transformed to k-space using the backscattering amplitudes, and phase-shift functions of Fe-O were extracted by the FEFF 7.0 (Zabinsky et al., 1995) based on the structure of $FeSiO_3$ ferrosilite. Curve fitting analysis was performed for the first shell (Fe-O).

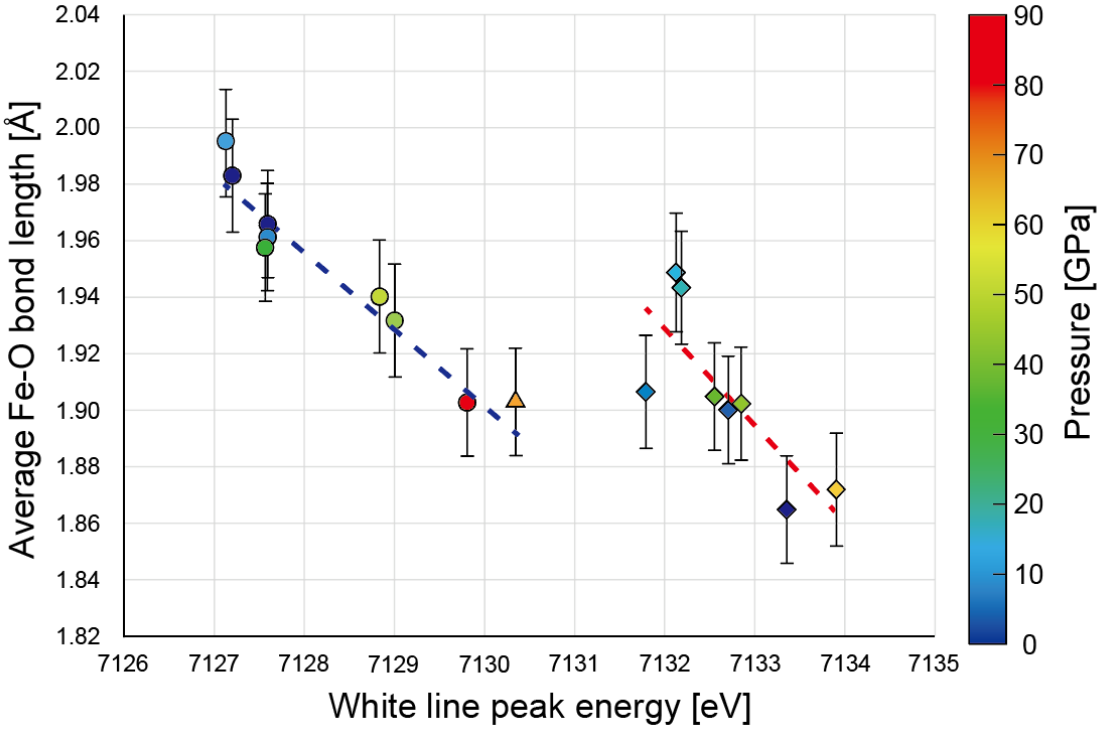

Figure S1. The peak energy of the white line vs. the average Fe^{2+}-O (circles, reduced glass; triangle, W-doped glass used in Ozawa et al., 2021) and Fe^{3+}-O bond lengths (diamonds, oxidized glass).

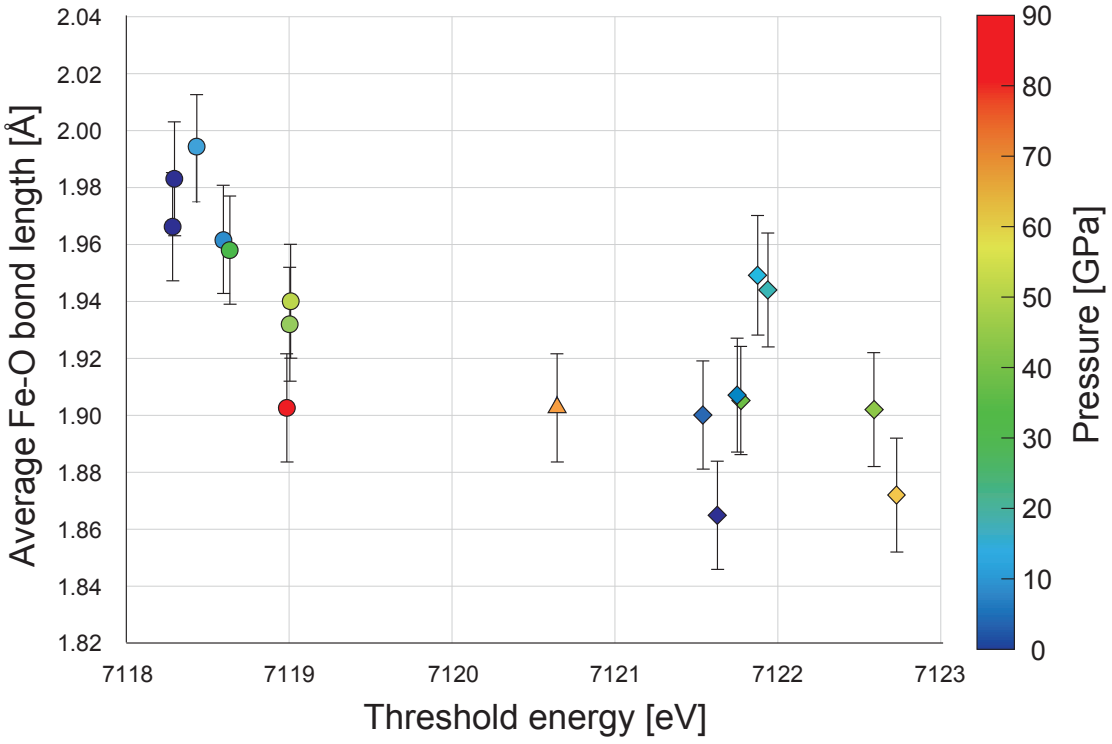

Figure S2. The threshold energy vs. the average Fe^{2+}-O and Fe^{3+}-O bond lengths. Symbols are the same as those in Figure S1.

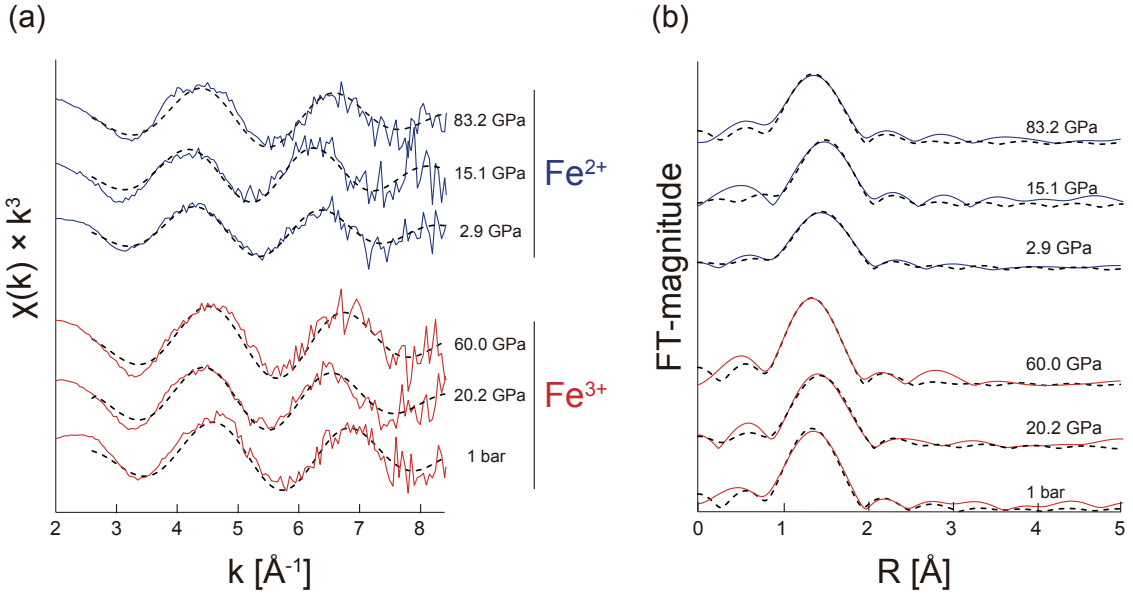

Figure S3. EXAFS oscillations and radial structure functions of Fe in the reduced (blue) and oxidized (red) basaltic glasses. (a) k^3-weighted oscillations, $\chi(k) \times k^3$, extracted from EXAFS spectra. (b) The radial structural function at the K-edge for Fe which was Fourie transformed (FT) from k^3-weighted EXAFS oscillations in (a). The black dashed curves in (a) and (b) show simulation data of EXAFS spectra using a parameter extracted by FEFF 7.0.

Table S1

Chemical Compositions of Reduced and Oxidized Basaltic Glasses

wt%	Reduced glass	Oxidized glass
SiO_2	49.50(35)	50.33(58)
TiO_2	1.09(5)	1.13(6)
Al_2O_3	14.68(11)	14.77(13)
FeO*	9.53(13)	10.39(12)
MgO	8.42(11)	8.45(9)
CaO	9.52(3)	9.36(11)
Na_2O	2.89(16)	3.39(7)
K_2O	0.12(2)	0.14(3)
Total	95.76	97.97

The values in parentheses represent one standard deviations in the last digits.

*total Fe as FeO.

Table S2

Pre-edge, XANES, and EXAFS Data for Reduced and Oxidized Basaltic Glasses

		Pre-edge		XANES		EXAFS	
	Pressure (GPa)	Centroid (eV)	Intensity	Threshold energy (eV)	Peak Energy (eV)	k range	Fe-O bond length (Å)
Reduced glass	1 bar	7111.92	0.1381	7118.30	7127.20	2.6–8.4	1.983 (20)
	2.9	7111.91	0.1200	7118.28	7127.58	2.6–8.4	1.966 (19)
	8.7	7112.09	0.1313	7118.60	7127.59	2.6–8.4	1.962 (19)
	15.1	7111.92	0.1248	7118.43	7127.13	2.6–8.4	1.995 (18)
	27.3	7111.79	0.0970	7118.64	7127.55	2.6–8.4	1.958 (19)
	46.9	7111.89	0.0968	7119.00	7128.99	2.6–8.4	1.932 (20)
	52.0	7111.91	0.1021	7119.01	7128.83	2.6–8.4	1.940 (20)
	67.6*	7112.01	0.0873	7120.64	7130.34	2.6–8.4	1.904 (19)
	83.2	7111.76	0.1044	7118.98	7129.81	2.6–8.4	1.903 (19)
Oxidized glass	1 bar	7113.40	0.2665	7121.63	7133.36	2.6–8.4	1.865 (19)
	3.3	7113.40	0.2332	7121.54	7132.70	2.6–8.4	1.900 (19)
	7.6	7113.39	0.2071	7121.75	7131.79	2.6–8.4	1.907 (20)
	16.2	7113.32	0.1514	7121.88	7132.13	2.6–8.4	1.949 (21)
	20.1	7113.34	0.1578	7121.94	7132.19	2.6–8.4	1.944 (20)
	38.2	7113.26	0.1312	7121.77	7132.56	2.6–8.4	1.905 (19)
	43.6	7113.30	0.1449	7122.59	7132.85	2.6–8.4	1.902 (20)
	60.0	7113.20	0.1420	7122.73	7133.91	2.6–8.4	1.872 (20)

The values in parentheses represent one standard deviations in the last digits. Uncertainties in the pre-edge intensity and the centroid energy are ±10% and ±0.1 eV, respectively.

*Reduced W-doped glass used in Ozawa et al. (2021).